

## A new 200 Ma paleomagnetic pole for Africa, and paleo-secular variation scatter from Central Atlantic Magmatic Province (CAMP) intrusives in Morocco (Ighrem and Foug Zguid dykes)

A. Palencia-Ortas,<sup>1</sup> V. C. Ruiz-Martínez,<sup>1</sup> J. J. Villalaín,<sup>2</sup> M. L. Osete,<sup>1</sup> R. Vegas,<sup>3</sup> A. Touil,<sup>4</sup> A. Hafid,<sup>4</sup> G. McIntosh,<sup>1</sup> D. J. J. van Hinsbergen<sup>5</sup> and T. H. Torsvik<sup>5,6,7</sup>

<sup>1</sup>Departamento de Física de La Tierra, Astronomía y Astrofísica I, Facultad de Física, Universidad Complutense de Madrid, Avda. Complutense s/n, 28040 Madrid, Spain. E-mail: vcarlos@fis.ucm.es

<sup>2</sup>Departamento de Física, Escuela Técnica Superior, Universidad de Burgos, Avda. Cantabria s/n, 09006 Burgos, Spain

<sup>3</sup>Departamento de Geodinámica, Facultad de Geología, Universidad Complutense de Madrid, Spain

<sup>4</sup>Département des Sciences de la Terre, Faculté des Sciences et Techniques, Guéliz BP 548 Marrakech, Morocco

<sup>5</sup>Physics of Geological Processes (PGP), University of Oslo, Sem Sælands vei 24, NO-0316 Oslo, Norway

<sup>6</sup>Center for Geodynamics, Geological Survey of Norway (NGU), Leiv Eirikssons vei 39, 7491 Trondheim, Norway

<sup>7</sup>School of Geosciences, University of the Witwatersrand, WITS 2050 Johannesburg, South Africa

Accepted 2011 March 10. Received 2011 February 13; in original form 2010 July 6

### SUMMARY

Available apparent polar wander (APW) paths for the 200 Ma configuration of Pangea, just prior to the opening of the Central Atlantic Ocean, differ as much as 10° in arc length. Here, we add new data from northwest Africa for this time, obtained from the northeast-trending Foug-Zguid and Ighrem dykes (*ca.* 200 Ma). These dykes form part of the northern domain of the Central Atlantic Magmatic Province (CAMP), and crosscut the Anti-Atlas Ranges in Morocco, and compositionally correspond to quartz-normative tholeiites intruded in continental lithosphere shortly before the opening of the Central Atlantic Ocean. The Foug-Zguid dyke has been intensively studied, whereas the Ighrem dyke has received less scientific focus. We sampled both dykes for paleomagnetic investigation along 100 km of each dyke (12 sites for Foug-Zguid and 11 for Ighrem, 188 samples included in the final analyses). Rock magnetic experiments indicate a mixture of multidomain and single-domain magnetite and/or low-Ti titanomagnetite particles as the principal remanence carriers. In both dykes, the primary nature of the characteristic remanent magnetization is supported by positive contact tests, related to Fe-metasomatism or baked overprints of the corresponding sedimentary country rocks. The directions of the characteristic magnetization exhibit exclusively normal polarity. Site-mean virtual geomagnetic poles are differently grouped in each dyke, suggesting distinct geomagnetic secular variation records. The Foug-Zguid paleomagnetic pole ( $N = 12$ ,  $PLat = 67.9^\circ N$ ,  $PLon = 247.9^\circ E$ ,  $\kappa = 125$ ,  $A_{95} = 3.9^\circ$ ) plots close to that of Ighrem ( $N = 11$ ,  $PLat = 78.4^\circ N$ ,  $PLon = 238.2^\circ E$ ,  $\kappa = 47$ ,  $A_{95} = 6.7^\circ$ ), confirming those mineralogical and geochemical evidences supporting that they represent dissimilar magmatic stages. Virtual geomagnetic poles dispersion from both dykes ( $S = 10.5_{8.1}^{13.0}$ ) is in line with those obtained from recent studies of a CAMP-related dyke in Iberia and results from CAMP lavas in the Argana basin. These three new estimates of paleosecular variation at low latitudes around the Triassic–Jurassic boundary are concordant with a recently proposed dispersion curve for the Jurassic but suggest a slightly lower geomagnetic scatter than considered so far. After combining results from both dykes, the resulting paleomagnetic pole ( $PLat = 73.0^\circ N$ ,  $PLon = 244.7^\circ E$ ,  $N = 23$ ,  $\kappa = 55$ ,  $A_{95} = 4.1^\circ$ ) is statistically compared with existing and coeval African paleopoles, and with global synthetic 200 Ma running mean poles in northwest Africa coordinates.

**Key words:** Plate motions; Palaeomagnetic secular variation; Palaeomagnetism applied to tectonics; Rock and mineral magnetism; Cratons; Africa.

## 1 INTRODUCTION

Several paleomagnetic studies have been carried out in uppermost Triassic–lowermost Jurassic rocks from Africa, but in the most recent apparent polar wander (APW) paths (Besse & Courtillot 2002; Torsvik *et al.* 2008; hereafter referred as to BC2002 and T2008 APWPs, respectively) there are still few high quality ~200 Ma paleopoles for the African Plate. A key to overcome this shortcoming is to obtain data from ‘stable’ Africa, as many of the poles come from ‘old’ studies that do not meet current experimental standards.

The dykes of Fom-Zguid (FZ; Leblanc 1973; Sebai *et al.* 1991) and Ighrem (IG; Touil *et al.* 2008) in Morocco (subsequently named FZ and IG dykes, respectively; Fig. 1) form part of the African expressions of the northern domain of the so-called Central Atlantic Magmatic Province (CAMP). The mafic dykes and sills, and the tholeiitic surface basalts of the ~200 Ma CAMP are spread over at least 7 million km<sup>2</sup> across North and South America, West Africa and southwestern Europe, centred upon, but extending far beyond the initial Pangean rift zone that developed into the Central Atlantic Ocean (Marzoli *et al.* 1999). The northern domain of the CAMP is characterized by large, NE trending, extrabasinal dykes occurring in the Iberian Massif, the Anti-Atlas Ranges of Morocco and the coastal plain of the Canadian Maritime Provinces. They are quartz-normative tholeiites intruded into continental lithosphere prior to the opening of the Central Atlantic Ocean (May 1971) that started at around 195 Ma (Labails *et al.* 2010).

Some preliminary paleomagnetic work has been performed at the FZ dyke but no previous paleomagnetic information is available for the IG dyke. Hailwood & Mitchell (1971) carried out a pioneering paleomagnetic study of five sites from the FZ dyke, but the study does not meet today’s quality criteria. Recent paleomagnetic investigations of CAMP units have been performed in North America (Olsen *et al.* 2003), Brazil (De Min *et al.* 2003; Ernesto *et al.* 2003), Iberia (Palencia-Ortas *et al.* 2006) and Morocco (e.g. Palencia-Ortas 2004; Knight *et al.* 2004; Ruiz-Martinez *et al.* 2007). Knight *et al.* (2004) studied 66 lavas and sediments from the High Atlas, but they concluded that their pole did not represent an ‘African pole’ because it does not adequately average secular variation of the Earth’s magnetic field.

Investigations of the baked contacts, including rock magnetic characterizations of both the country rock and the thick FZ dyke margins, as well as anisotropy of the magnetic susceptibility (AMS), were previously reported for some of the sites presented in this paper (Silva *et al.* 2004; 2006a,b). Silva *et al.* (2006b) obtained a positive contact-test that is mainly related to Fe-metasomatism in the host sedimentary rocks during magma intrusion and cooling. They also studied six FZ sites mainly collected at the margin of the dyke, where obliteration of the primary mineralogy is observed (Touil *et al.* 2008) and remagnetizations due to weathering or hydrothermal activity obscure and may replace the original emplacement magnetization (see also Palencia-Ortas *et al.* 2006 for a discussion). Silva *et al.* (2006b) found several remagnetizations but also Characteristic Remanent components (ChRc) directions close to those of Palencia-Ortas (2004) from the central part of the FZ dyke. They therefore concluded that ‘the paleomagnetic pole obtained by Palencia-Ortas (2004) is related to the Earth magnetic field during intrusion and can be considered as a well-constrained paleomagnetic pole for Africa 197 Ma. However, the limited number of sites available to compute a FZ paleomagnetic pole could be a drawback for such a conclusion. The positive contact test obtained by Silva *et al.* (2006b) confirmed that the age of magnetization is the same as the age of the dyke, but unresolved issues remain, such as including the extent to which the remagnetizations were contributing to the isolation of the ChRc and whether the dyke was intruded during such a short time interval that geomagnetic secular variation may not have been averaged.

In this new paleomagnetic study, we present new data from the FZ dyke increasing the number of sites studied by Palencia-Ortas (2004) to 12 sites, all collected in its central part with respect to the margins. These data characterize the magnetic properties of these FZ dyke samples and resolve a high-quality FZ paleomagnetic pole. In addition, we present the first rock magnetic and paleomagnetic results from the IG dyke (11 sites), as well as from its sedimentary host rocks (of Precambrian age, Thomas *et al.* 2004). A positive baked contact test and a new IG palaeopole are presented. Then we compare FZ to IG paleopoles, as well as with (i) previous preliminary paleomagnetic FZ results; (ii) the 20 Ma window running mean pole centred at 200 Ma of the BC2002 and T2008 APWPs (which differ in the paleomagnetic data selection and the plate

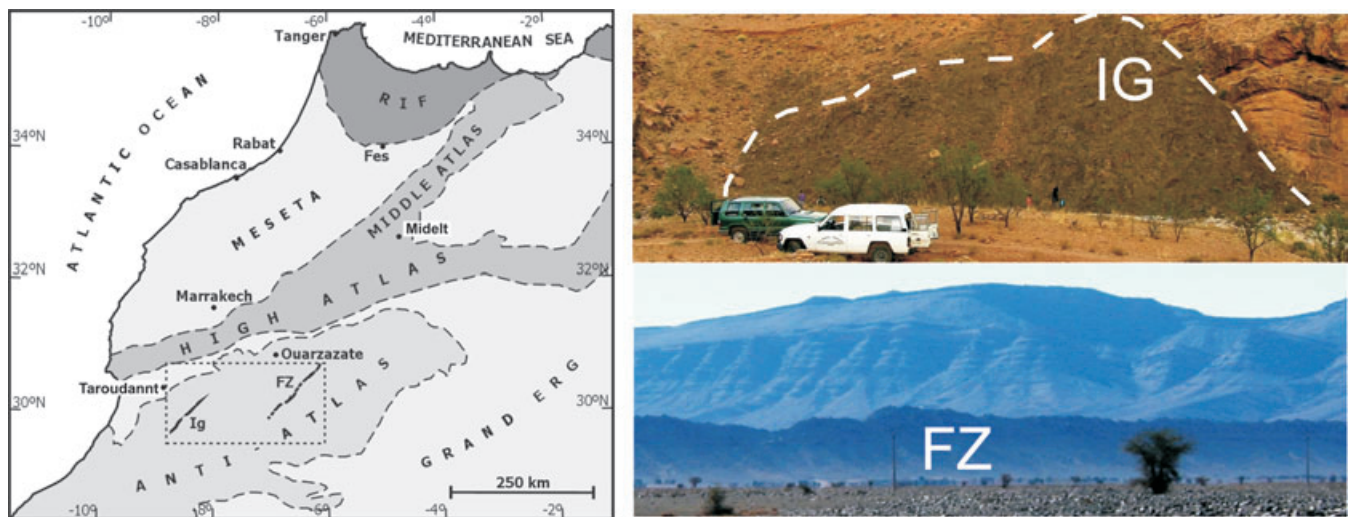


**Figure 1.** Left-hand panel: simplified sketch showing the main tectonic units of Morocco and the location of the studied Ighrem (IG) and Fom Zguid (FZ) dykes. Right-hand panel: photographs of the IG dyke intruding Precambrian sediments (showing a dotted white-outline sketch of the dyke contact), and of the prominent FZ dyke (foreground) and the Paleozoic sediments (background).

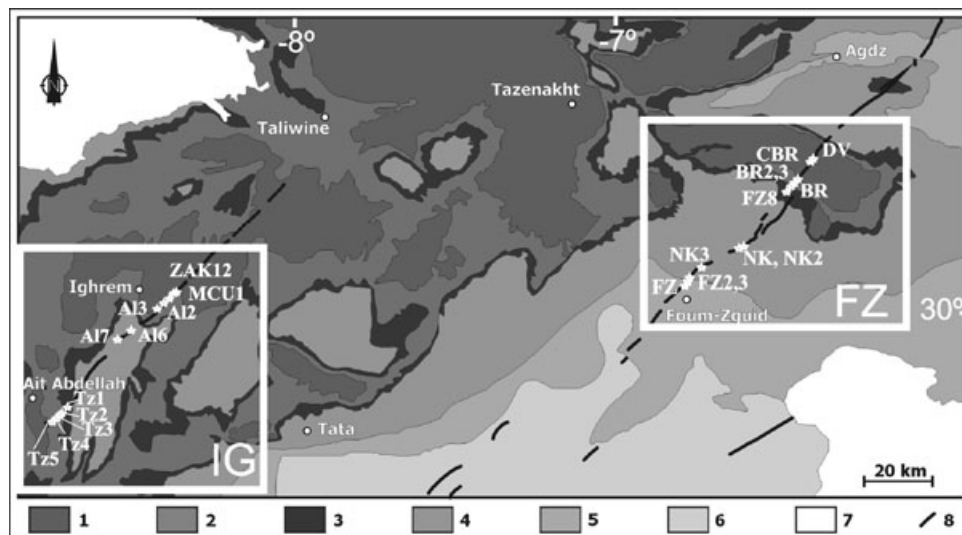


**Figure 2.** Simplified geological map of the studied area (central Anti-Atlas) showing the location and code name of the sampled sites from the studied IG and FZ dykes. 1: Precambrian formations; 2: Ediacarian (Adoudounian); 3: Late Ediacarian (Taliwinian); 4: Cambrian; 5: Ordovician-Silurian; 6: Devonian; 7: post-Paleozoic cover; 8: Mesozoic dolerite dykes.

circuits used), transferred to northwest African coordinates and (iii) those individual African paleomagnetic poles obtained from igneous and sedimentary rocks with ages ranging between 190 and 210 Ma which are included in the BC2002 or T2008 compilations. Finally, the results of these comparisons and the reliability of these poles are discussed.

## 2 GEOLOGICAL SETTING AND AGE OF THE STUDIED MOROCCAN INTRUSIONS

### 2.1 Foum-Zguid and Ighrem dykes

The FZ and IG dykes are subvertical, NE–SW trending, CAMP-related dolerite dykes located in southern Morocco (Figs 1 and 2). Contact metamorphism is observed at the intruded formations (Youbi *et al.* 2003). The dykes traverse the Hercynian-folded Precambrian and Paleozoic strata of the Anti-Atlas, an area that has remained tectonically stable since the end (*ca.* 300 Ma) of the Hercynian orogeny (e.g. Marçais & Choubert 1956; Burkhard *et al.* 2006), with some recent uplift partly ascribed to the occurrence of a high-temperature mantle anomaly in Neogene times (Frizon de Lamotte *et al.* 2009).

The exceptionally well exposed (Fig. 1) and intensively studied FZ dyke is one of the major dykes of the Anti-Atlas domain. It has an overall length of about 200 km (from the village of Foum Zguid in the southwest to Jbel Saghro in the northeast) and is 100–150 m wide, forming a continuous crest amid surrounding Paleozoic sedimentary rocks (Fig. 2). It consists of tholeiitic dolerite with a subophitic texture and micropegmatitic quartz-potassium feldspar residue (Leblanc 1973; Michard 1976; Schermerhorn *et al.* 1978; Bertrand 1991; Aarab *et al.* 1994). Sebai *et al.* (1991) determined a plagioclase  $^{40}\text{Ar}/^{39}\text{Ar}$  non-plateau age of  $196.9 \pm 1.8$  Ma.

The IG dyke (Fig. 1) is another of the main intrusive bodies in the Anti-Atlas domain, but it has not been the subject of any mineralogical or geochemical study, excepting that of Touil *et al.* (2008). These authors named it the ‘IG dyke’ after the nearest eponym main village in Southern Morocco, although it is also was previously referred as the ‘Asdrem dyke’ (Youbi *et al.* 2003). It runs parallel

to the FZ great dyke, extending over almost 200 km between Ait Abdellah and Taliwine villages, from east of the Kerdous inlier in the south to the Siroua Massif in the north. It crosscuts at high angle the different Precambrian and lower Paleozoic formations of the western Anti-Atlas (Fig. 2). The dyke was intruded along vertical Hercynian fractures, and its width varies from 60 to 150 m (Youbi *et al.* 2003). Unlike the FZ dyke, the IG dyke is often covered by Neogene and Quaternary deposits and appears segmented and highly weathered, occupying the *tahlwegs* (valley ways) oriented along its trace. Good exposure is rare and situated to the northwest of the Ait Abdallah uplifted inlier, where the outcrops contain fresh rocks (Touil *et al.* 2008). The IG dyke has remained undated and is vaguely referred to as ‘Hercynian magmatism’ despite its orientation. However, the IG dyke is ascribed to the CAMP as it is petrologically and structurally similar to the FZ dyke (Touil *et al.* 2008), and further chronological studies are in progress to verify its radiometric age. The available mineralogical and geochemical analyses for the IG dyke (Touil *et al.* 2008) differ from those presented by the Foum Zguid (Bertrand *et al.* 1982; Bertrand 1991) and Messejana-Plasencia (Cebriá *et al.* 2003) dykes. The IG dyke analyses show a contrasted evolution of the compositions that is marked by the increase in  $\text{Fe}_2\text{O}_3$ ,  $\text{TiO}_2$ ,  $\text{P}_2\text{O}_5$ ,  $\text{K}_2\text{O}$ , Ba, Nb and Ce contents and the decrease in  $\text{Al}_2\text{O}_3$ , MgO and CaO during crystallization (compared to the FZ and Messejana-Plasencia dykes). On the contrary, taking into account its constant and low MgO content, the IG rocks are thus comparatively richer in  $\text{Fe}_2\text{O}_3$ ,  $\text{TiO}_2$ ,  $\text{P}_2\text{O}_5$  and  $\text{K}_2\text{O}$  and trace incompatible elements, and poorer in  $\text{Al}_2\text{O}_3$ , CaO (Figs 6 and 7 from Touil *et al.* 2008). This means that although all three dykes belong to the CAMP, the IG dyke is magmatically the most evolved (Touil *et al.* 2008).

### 2.2 Moroccan CAMP volcanism

The number of CAMP geochronological data has increased over recent years, although new Moroccan data come from basaltic flows, and not intrusives. Nomade *et al.* (2007) reviewed and selected available  $^{40}\text{Ar}/^{39}\text{Ar}$  data, accepting 37 ages for African CAMP magmatism that ranged from  $202.5 \pm 3.0$  to  $190.5 \pm 1.2$  Ma (‘older’ data of Sebai *et al.* 1991 were not included because of calibration

problems with the applied LP6 biotite monitor). In the Moroccan central High Atlas and Oujda basins, Verati *et al.* (2007) reported CAMP  $^{40}\text{Ar}/^{39}\text{Ar}$  plateau ages ranging from  $197.8 \pm 0.7$  to  $201.7 \pm 2.4$  Ma (with a restricted peak at  $199.1 \pm 1$  Ma) for the main tholeiitic basaltic event, followed by a younger, small volume episodic eruption of magmas (mean age of  $196.6 \pm 0.6$  Ma).

Using geochronological, magnetostratigraphic (the reversed polarity chron E23r) and geochemical correlations between CAMP subprovinces, Marzoli *et al.* (2004) and Knight *et al.* (2004) suggested a short duration for the peak CAMP activity of less than 1 Ma (with an  $^{40}\text{Ar}/^{39}\text{Ar}$  age of  $199.1 \pm 1.0$  Ma) and concluded that CAMP volcanism in Morocco erupted across the Triassic–Jurassic (T–J) boundary. Milankovitch cyclostratigraphy was used by Whiteside *et al.* (2007) to correlate the onset in Morocco (Argana basin and central High Atlas) with that in eastern North America (Newark and Fundy basins), where the total duration of the CAMP volcanic event is constrained to  $\sim 610$  ky. Recently, high precision  $^{206}\text{Pb}/^{238}\text{U}$  zircon CAMP data of  $201.38 \pm 0.31$  Ma has been reported (Schoene *et al.* 2010) at the North Mountain Basalt (Fundy basin) correlating this volcanism and the end-Triassic mass extinction. According to the trans-Atlantic CAMP multidisciplinary correlation of Deenen *et al.* (2010), the onset of CAMP volcanism in Morocco (Argana basin) is proposed to occur  $\sim 20$  ka after the chron E23r, prior to the T–J boundary. Only normal polarities were observed in lava flows from the Argana basin (Ruiz-Martínez *et al.* 2007).

Analytical resolution of the geochronological data is not yet precise enough for the timing of the T–J boundary, or even for estimating the relatively short CAMP volcanic activity duration. In contrast, and despite the absence of temporal correlations between Moroccan CAMP volcanism and intrusions, uncertainties on the order of 1 to few Ma are not problematic for our paleomagnetic purposes. IG and FZ CAMP dykes are reasonably ascribed to an age of *ca.* 200 Ma. In fact, their time span are quite precise as they will be compared with 20 Ma APWP running windows centred at 200 Ma and with individual paleopoles of latest Triassic–earliest Jurassic age.

### 3 FIELD SAMPLING AND LABORATORY MEASUREMENTS

A total of 23 sites from the central parts of the IG and FZ dykes (11 and 12 sites, respectively) spanning 100 km of each dyke have been sampled (Fig. 2). In addition, host sedimentary Precambrian rocks close to the IG dyke margins (site TZ5, Figs 1 and 2) were sampled to perform a baked contact test. Samples were cored (2.54 cm in diameter) with a portable gasoline-powered drill and oriented using an inclinometer and a magnetic compass. Cores were cut in the laboratory into standard specimens (2.2 cm length) for paleomagnetic measurements. Alternating field demagnetized specimens, core chips and core end pieces were used for rock magnetic experiments.

Measurements were made in the Paleomagnetic laboratory and the Physical Techniques Center of the Complutense University in Madrid and in the Paleomagnetic laboratory of the University of Burgos. Low-field magnetic susceptibility ( $\chi$ ) was measured using an AGICO KLY-3 susceptibility meter. Remanence measurements (natural and isothermal, NRM and IRM, respectively) were made using an AGICO JR5-A spinner and 2G cryogenic (model 755 DC SQUID) magnetometers. IRM was imparted using an ASC Scientific IM10-30 impulse magnetizer. Magnetic hysteresis measure-

ments were made using a coercivity meter (Jasonov *et al.* 1998). Low-temperature IRM curves were measured using a Quantum Design MPMS-XL squid magnetometer. Thermal (TH) and alternating field (AF) demagnetization of NRM and IRM were carried out using Schonsted Instruments THD-1, AFD-1 and ASC TD48-SC demagnetizers.

### 4 ROCK MAGNETIC RESULTS

Representative samples were subjected to stepwise IRM acquisition up to 2 T, applying at least 16 field steps. Subsequently, thermal demagnetization of orthogonal IRMs (Lowrie 1990, applying fields of 2, 0.4 and 0.12 T) was carried out. All samples displayed a similar behaviour, approaching saturation below 0.3 T. The 0.12 T IRM component was completely demagnetized by 575–600 °C, suggesting magnetite, possibly partially oxidized, as the low coercivity mineral (Figs 3a and b and 4a and b). In some cases, a decrease in magnetization was observed around 350–400 °C (Fig. 3b), which may indicate the presence of maghemite. In only a few cases did the 0.4 and 2 T components contribute significantly to the IRM, with unblocking temperatures over 600 °C probably indicating haematite. There was no evidence for unblocking of the 0.4 and 2 T components below 150 °C, so that contribution of goethite to the remanence can be discounted.

Hysteresis parameters were obtained for selected samples in a maximum applied field of 0.5 T. Closed loops, saturation of the ferromagnetic grains and little or no paramagnetic/diamagnetic high-field contributions were observed. Both the induced ( $M_i$ ) and remanent ( $M_r$ ) magnetization curves were dominated by low coercivity (<0.3 T) minerals (Figs 3c and 4c), in agreement with the IRM results. The data fell within the upper left part of the pseudo-single-domain region of a Day plot (Figs 3d and 4d; Day *et al.* 1977), closely following the trends for single- and multidomain mixture of magnetite or low-Ti titanomagnetite (Dunlop 2002).

Low-temperature IRM curves were measured for FZ representative samples. A 4 K IRM, acquired in a 5 T applied field, was measured during zero-field warming to room temperature. A large drop in remanence around 110 K was observed, due to the Verwey transition associated with magnetite (Fig. 3e).

In summary, rock magnetic experiments suggest a magnetic mineralogy dominated by a mixture of single-domain and multidomain grains of nearly pure magnetite or low-Ti titanomagnetite. This is in close agreement with the findings of Silva *et al.* (2004), who performed complementary rock magnetic investigations on FZ dyke margin sites (Curie curves, microscopic studies), and with the petrographic observations of Touil *et al.* (2008) at the IG dyke indicating the presence of titanomagnetite in the primary minerals assemblage.

### 5 PALEOMAGNETIC RESULTS

#### 5.1 Foun-Zguid dyke

A large scatter in both initial NRM directions and intensities was observed. Intensity values typically ranged between  $4 \times 10^{-2}$  and  $3 \text{ Am}^{-1}$ , with some specimens exhibiting anomalously high intensities (up to  $342 \text{ Am}^{-1}$ ). Initial NRM intensities  $NRM_0$  versus  $\chi$  are plotted in Fig. 3(f), together with the Koenigsberger values (Stacey 1967; Dunlop *et al.* 1984),  $Q_n$ , which quantify the ratios between the remanent and induced magnetizations ( $Q_n = NRM_0/(\chi H)$ ,  $H$  is the geomagnetic field intensity =  $39 \text{ Am}^{-1}$ ). The values obtained were generally consistent with a thermoremanent (TRM) origin for

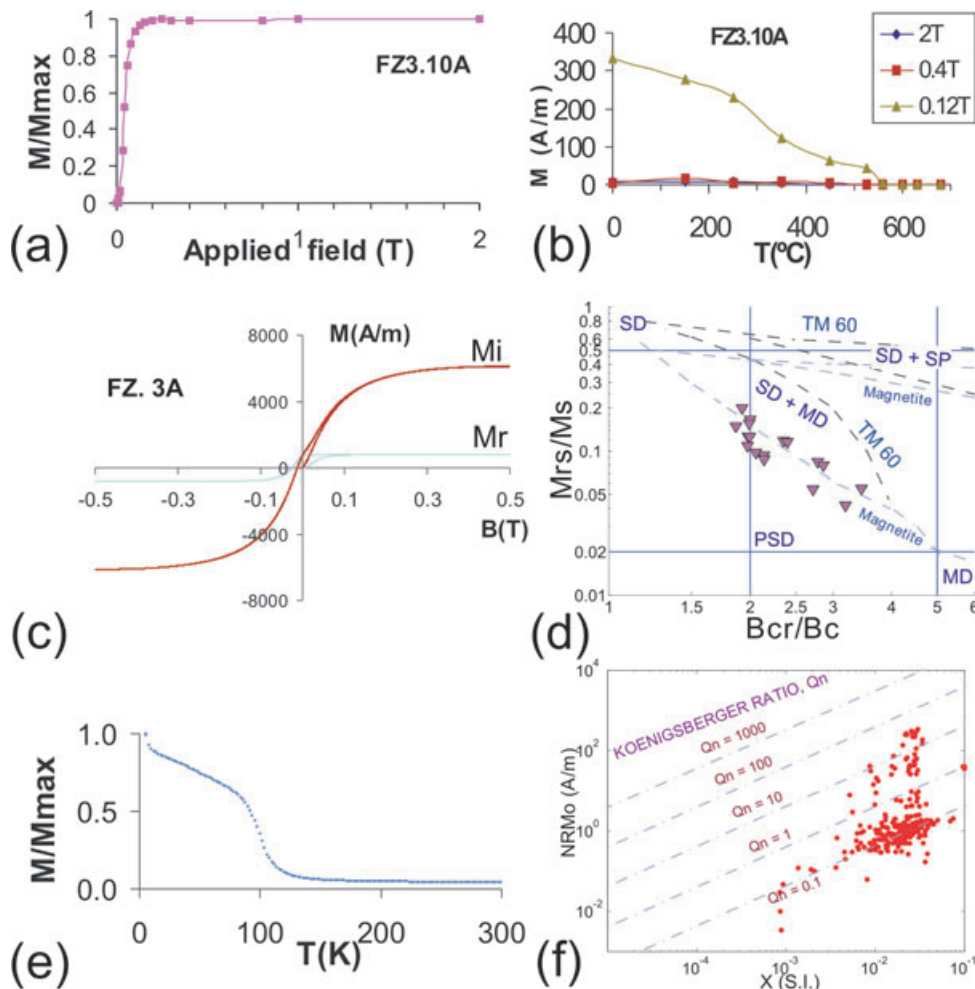


**Figure 3.** Representative rock magnetic results from FZ dyke. (a) IRM acquisition curve and (b) thermal demagnetization of orthogonal IRM components. (c) Hysteresis curve: remanent ( $M_r$ ) and induced ( $M_i$ ) magnetizations. (d) Hysteresis parameters of all samples, along with theoretical curves for mixtures of single domain (SD), multidomain (MD) and superparamagnetic (SP) magnetite and 60 per cent Ti-titanomagnetite (TM60) grains (Dunlop 2002). (e) Saturation IRM acquired at 4 K monitored during zero field heating to room temperature. (f) Koenigsberger ratio,  $Q_n$ , of all FZ samples.

the NRM, but high ratios ( $Q_n > 10$ ) and dispersed NRM directions also suggest the presence of IRMs acquired by lightning strikes. The predominantly high positive relief of the FZ dyke with respect to the country rock may explain the relative importance of lightning strikes.

Detailed stepwise thermal (TH) and alternating (AF) demagnetization techniques were applied to 2–4 pilot specimens per site. One or two magnetic components were observed, with different degrees of overlap. Specimens with high  $Q_n$  ratios ( $Q_n > 10$ ) were rejected from the paleomagnetic study because their NRMs were completely remagnetized (Fig. 5a) or their high NRM intensities might have disturbed the field sampling orientation when using the magnetic compass. From a total of 296 specimens, 120 independently oriented samples (12 sites) were selected for demagnetization and directional analyses.

In some cases, only one stable component was observed (Fig. 5b). In most cases, a low coercivity component with highly scattered directions overlapped with a second, higher coercivity component (Fig. 5c). This component always showed well grouped, normal polarity directions, and is interpreted as the ChRc. When two components were observed, AF demagnetization was usually more effective than TH demagnetization in isolating the ChRc. Therefore, AF demagnetization was used as the routine demagnetization

technique, with at least eight steps up to a maximum of 80–100 mT. Median destructive fields ranged between 5 and 20 mT. Maximum unblocking temperatures ranged between 450 and 575–600 °C.

When the low coercivity phase exhibited anomalously high intensities we have interpreted this as a lightning-induced IRM. There have been few cases without anomalous initial NRM values in which it could be due to chemical alteration, hydrothermal and/or viscous magnetization effects. In the absence of petrographic or viscosity investigations, we are unable to distinguish between these possibilities. In spite of this, the magnetic behaviour during NRM demagnetization of the samples from the central part of the dyke stands out in contrast to the complexity of the remanence of the samples of the margin of the same dyke (Silva *et al.* 2006b), where several directional magnetic components were found. These authors did not find indication of lightning effects but described (i) a low-temperature component, probably a viscous remanent magnetization (VRM); (ii) an intermediate component (sometimes close to the recent field, sometimes not) that could correspond to a chemical remanent magnetization (CRM) related to the presence of maghemite; and (iii) a highest temperature component (above 500 °C) associated with the ChRc. The widespread CRM acquired since late Tertiary times in the Sahara region (Henry *et al.* 2004), that according to Silva *et al.* (2006b) could likely be responsible of these directions from the FZ

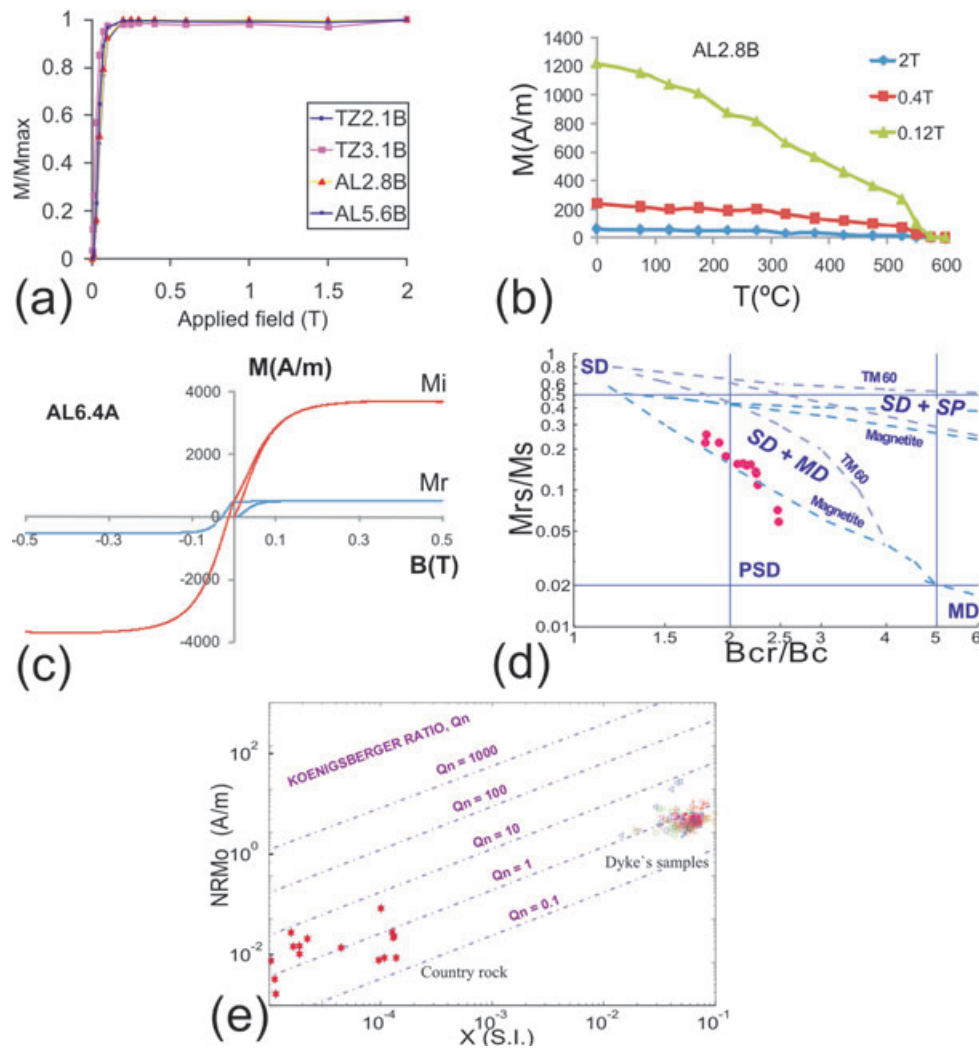


**Figure 4.** Representative rock magnetic results from IG dyke. (a) IRM acquisition curve and (b) thermal demagnetization of orthogonal IRM components. (c) Hysteresis curve: remanent ( $M_r$ ) and induced ( $M_i$ ) magnetizations. (d) Hysteresis parameters of all samples, along with theoretical curves for mixtures of single domain (SD), multidomain (MD) and superparamagnetic (SP) magnetite and 60 per cent Ti-titanomagnetite (TM60) grains (Dunlop 2002). (e) Koenigsberger ratio,  $Q_n$ , of IG dyke and sedimentary country rock samples.

margins close to the recent field, it is not observed in the samples of the central part of the FZ dyke (this study).

Where possible, paleomagnetic directions were calculated from stable endpoints (with at least five linear steps) using principal component analysis (Kirschvink 1980) and site-mean directions were calculated using Fisher (1953) statistics (Fig. 5d). In cases where a high degree of overlapping was detected, principal component analysis was applied to fit (with at least eight planar steps) the corresponding plane that comprises both overlapped directions, and site-mean directions were calculated using the combined analysis of linear segments and remagnetization circles (McFadden & McElhinny 1988). Although it was possible to determine stable endpoint directions for some of these specimens, remagnetization circles were better defined after detailed AF demagnetization (Fig. 5e), and their convergence favoured by the random nature of the lightning-induced remagnetization, giving better results. For each site-mean direction, quantile–quantile plots of declination (inclination) against an assumed uniform (exponential) distribution supported Fisher-distributed directions. Site-mean directions (Table 1) were well grouped, with tectonically useful 95 per cent confidence intervals ( $1.8^\circ \leq \alpha_{95} \leq 8.4^\circ$ , geometric mean =  $4.4^\circ$ ) and precision

parameters ( $35 \leq k \leq 833$ , geometric mean = 133). The ChRc exhibited exclusively normal polarities (Fig. 7a).

### 5.2 Ighrem dyke

Initial NRM intensities (ranging from 0.9 to  $5.1 \text{ Am}^{-1}$  at dyke samples;  $2 \text{ Am}^{-1}$  on average) led to moderate  $Q_n$  ratios ( $Q_n \approx 1$ ), consistent with TRM values in both the dyke and the nearest country rock samples, with susceptibility and intensity ranges typical of igneous and sedimentary rocks, respectively (Fig. 4e). Initial NRM site-mean directions were generally well grouped, with the exception of some sites with visible signs of alteration. Unlike the FZ dyke samples, no evidence of lightning strikes is present in those from the IG dyke.

Two magnetic phases were distinguished after applying detailed, stepwise AF and TH demagnetization in specimens from the same sample. First, low coercivity/unblocking temperature component is isolated between 2 and 15 mT or 75–125 and 350–500 °C. Secondly, not overlapping, high coercivity/unblocking temperature component is isolated between 25 and 100 mT or 375–500 and 600 °C (Fig. 6a). The former directions have been interpreted as remagne-

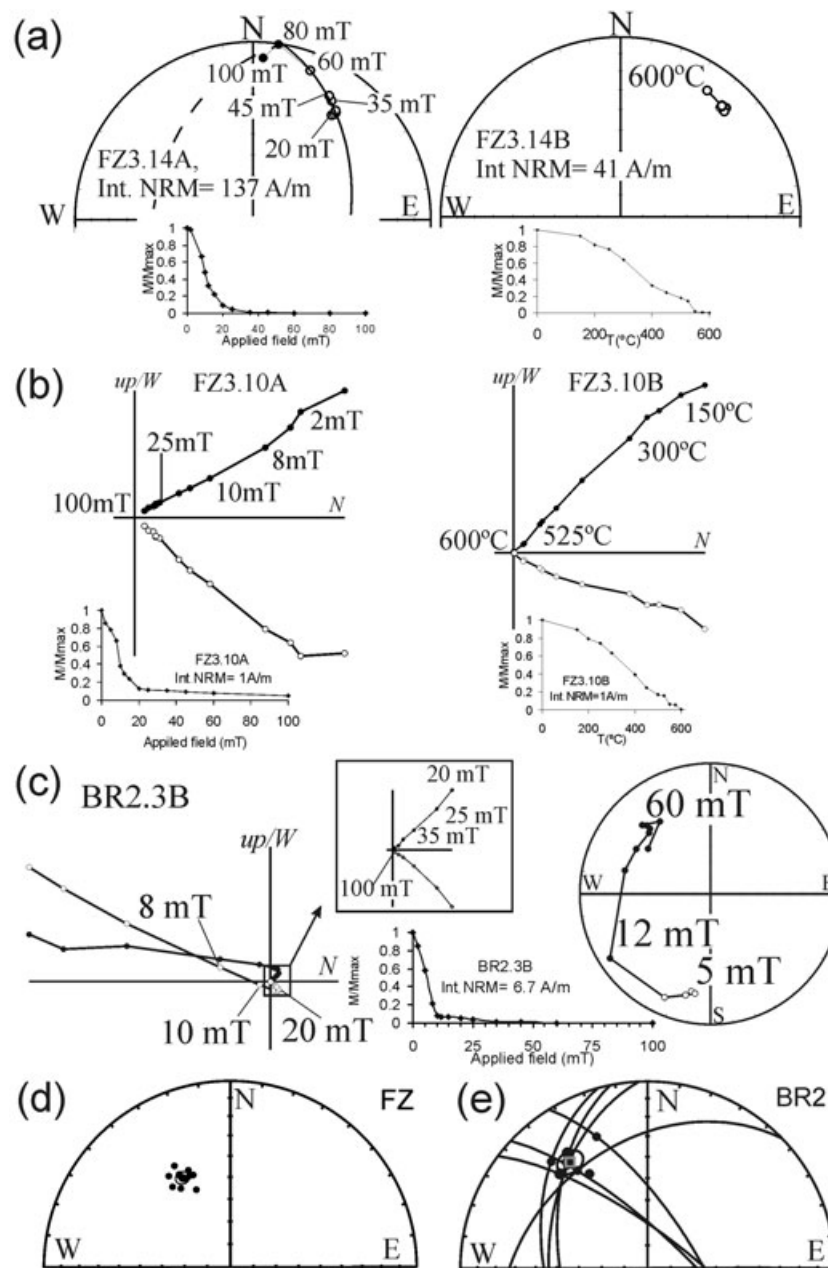


**Figure 5.** Orthogonal vector diagrams, equal area projections and normalized magnetization decays during AF and TH demagnetization of typical FZ dyke samples. (a) Rejected specimens (from the same sample, FZ3.14) exhibiting anomalously strong NRM due to lightning strikes. (b) Accepted specimens (the same sample, FZ3.10) with one stable component. (c) Accepted specimen (BR2.3B) with two overlapping components. Equal area projection of specimen and site-mean directions for (d) single component (FZ) and (e) two overlapped components (BR2).

tizations because their inclinations/declinations are systematically higher/closer to the present-day field than those from the latter corresponding directions. The remaining dyke samples were fully demagnetized by both TH and AF techniques. Median destructive fields ranged between 5 and 20 mT, and maximum unblocking temperatures were observed around 550–600°C. Principal component analysis was applied to calculate IG ChRes, using at least six linear steps of the high coercivity/unblocking temperature component and the origin, except in one of them where lines were combined with remagnetization planes. IG site-mean directions (Table 2) pass Fisherian distribution tests and show a slightly higher within-site dispersion ( $3.8^\circ \leq \alpha_{95} \leq 12.3^\circ$ , geometric mean =  $7.3^\circ$ ; 39  $\leq$

$k \leq 391$ , geometric mean = 128) than those observed at the FZ dyke. The IG dyke ChRes are all observed to be of normal polarity (Fig. 7c).

At the TZ5 site, the IG dyke intrudes folded Precambrian limestones (Thomas *et al.* 2004). Both limbs of the metre-scaled fold are clearly in contact with the *ca.* 60 m wide IG dyke (Fig. 1). The country rock was sampled at different distances from the dyke (from few centimetres to tens of metres) to perform a paleomagnetic baked contact test. Those country rock samples that are closest to the IG dyke (only some centimetres distant) have a single, linear magnetic component that is isolated at temperatures up to 550 °C (TZ5.20A, Fig. 6c). The direction of the component carried by the

**Table 1.** ChRc site-mean directions and VGPs from Fom Zguid and Ighrem dykes. *Site (D.T.):* Site code name and (AF, alternating field; TH, thermal) demagnetization technique (*D.T.*); *n*: number of independently oriented samples included in the analysis; *n<sub>L/P</sub>*: number of lines/planes calculated by principal component analysis; *SLat, SLon*: site location in latitude and longitude; *Dec, Inc*: declination and inclination; *k, α<sub>95</sub>*: precision parameter and semi-angle of 95 per cent confidence of directions; *PLat, PLon*: pole latitude and longitude. (*SLat, SLon, Dec, Inc, α<sub>95</sub>, PLat, PLon* in degrees).

Site (D.T.)	<i>n</i>	<i>n<sub>L/P</sub></i>	<i>SLat</i>	<i>SLon</i>	<i>Dec</i>	<i>Inc</i>	<i>k</i>	<i>α<sub>95</sub></i>	<i>PLat</i>	<i>PLon</i>
Fom Zguid										
fz (AF)	11	11/0	30.12	−6.88	331.8	44.8	257	2.9	65.0	261.6
fz2 (AF)	10	10/0	30.12	−6.88	341.5	36.9	211	3.3	70.8	237.6
fz3 (AF)	11	10/1	30.13	−6.87	331.8	36.5	153	3.7	62.8	248.6
nk3 (AF)	12	6/6	30.16	−6.84	332.9	41.6	52	6.3	65.1	255.2
nk (AF)	10	7/3	30.21	−6.73	338.8	41.1	35	8.4	70.0	249.0
nk2 (AF)	9	4/5	30.21	−6.73	339.3	47.8	122	4.9	72.0	264.3
FZ8 (AF)	7	7/0	30.35	−6.58	330.1	33.6	65	7.5	60.4	246.5
br (AF)	10	5/5	30.36	−6.57	340.4	40.7	135	4.3	71.2	246.0
br2 (AF)	11	4/7	30.37	−6.56	323.9	30.3	82	5.3	54.2	248.6
br3 (AF)	10	6/4	30.38	−6.55	348.1	37.6	350	2.7	75.8	225.2
cbr (AF)	10	0/10	30.43	−6.51	341.0	39.8	76	6.2	71.3	243.3
dv (AF)	9	8/1	30.44	−6.50	344.0	38.4	833	1.8	73.2	235.7
Ighrem										
ZAK12 (TH)	6	6/0	30.16	−8.28	348.6	53.1	69	8.1	79.7	284.6
MCU1 (TH)	6	6/0	30.09	−8.37	348.6	51.6	38	11.0	86.4	44.2
AL2 (AF)	8	5/3	30.09	−8.37	347.0	52.1	106	5.6	78.6	278.3
AL3 (TH)	6	6/0	30.07	−8.39	352.9	43.6	134	5.8	82.2	227.0
AL6 (TH)	6	6/0	30.03	−8.43	357.1	26.4	177	5.1	73.7	181.6
AL7 (TH)	6	6/0	30.03	−8.44	355.5	35.3	39	10.8	78.7	193.7
TZ1 (TH)	6	6/0	29.75	−8.72	343.1	37.2	82	7.4	72.3	234.7
TZ2 (AF)	8	8/0	29.75	−8.72	349.6	43.5	84	6.1	79.8	238.4
TZ3 (AF)	5	5/0	29.75	−8.71	321.0	47.9	39	12.3	56.2	270.0
TZ4 (AF)	4	4/0	29.76	−8.70	343.0	30.3	391	4.7	69.4	224.2
TZ5 (TH)	7	7/0	29.78	−8.67	348.6	37.2	252	3.8	76.3	222.8

immediate host sediments, calculated without applying any correction for their paleohorizontal restitution, is identical to that of the ChRc direction of the IG dyke samples at TZ5 (Fig. 6b). This total thermal remagnetization becomes a partial TRM with decreasing overprint temperatures as samples are increasingly distant from the dyke (see country rocks normalized magnetization decays during thermal demagnetization, Fig. 6c). Country rock samples located 6 m from the dyke show a normal polarity, low unblocking temperature (~350°C in TZ5.23A, Fig. 6c) directional component that is overlapped with a high unblocking temperature component of reversed polarity which is considered the ChRc of these sedimentary host rocks. After a detailed thermal demagnetization of these samples, the planes that contain the two directional unblocking temperature components describe remagnetization great circles in the equal-area demagnetization paths (TZ5.23A, Fig. 6c). A ChRc mean direction was calculated for the country rocks using the remagnetization great circles method, sometimes combining great circle and linear segment analysis as described by McFadden & McElhinny (1988). Reversed country rock ChRcs exhibited a higher grouping in their paleo-horizontal coordinates ( $n = 5$ ;  $Dec = 157.0$ ;  $Inc = -20.4$ ;  $\alpha_{95} = 11.8$ ), suggesting a pre-folding magnetization. The baked contact test indicates that the closest intruded sedimentary rocks are completely remagnetized by the thermal process due to the dyke intrusion. Precambrian host rocks are gradually less thermally affected in metre-scale distances from the IG dyke, preserving a pre-folding reversed polarity magnetization. The positive baked contact test support a primary ChRc direction of the IG dyke.

## 6 FOM-ZGUID AND IGHREM NEW PALEOPOLES AND RELIABILITY CRITERIA

Virtual geomagnetic poles (VGPs) for each site have been calculated for the FZ and IG dykes, together with their statistical parameters (Tables 1 and 2, Figs 7b and d). ‘Quantile–quantile’ plot tests were positive for each dyke, indicating that the VGPs were Fisher-distributed. Despite these results, which support that an incomplete resolution of ChRc can be excluded, an adequate averaging of geomagnetic secular variation in each dyke cannot be asserted.

The paleomagnetic pole obtained for the Fom Zguid dyke is:  $PLat = 67.9^\circ N$ ,  $PLon = 247.9^\circ E$ ,  $N = 12$ ,  $K = 125$  and  $A_{95} = 3.9^\circ$  (Tables 1 and 3). The paleopole obtained for the IG dyke is:  $PLat = 78.4^\circ N$ ,  $PLon = 238.2^\circ E$ ,  $N = 11$ ,  $K = 47$  and  $A_{95} = 6.7^\circ$  (Tables 2 and 3). FZ and IG paleopoles implies overlapping paleolatitudes at each site ( $22.4^\circ \pm 2.8^\circ$  and  $24.8^\circ \pm 5.0^\circ$ , respectively).

Van der Voo (1990) proposed seven criteria by which to reliably determine a paleomagnetic pole, giving rise to a quality factor  $Q$  ( $0 \leq Q \leq 7$ ) that can be assigned to the paleopole determination. A quality factor  $Q = 5$  has been ascribed to the determination of IG and FZ individual paleopoles because each of them meets at least the following reliability criteria of Van der Voo (1990): (1) well-determined age (for paleomagnetic purposes) of the rock unit (CAMP-affinity intrusion), (2) tectonic coherence—it is younger than the last tectonic phase that affected northwest African craton area of the dyke emplacement, (3) positive contact test constraining the age of the magnetization, (4) adequate demagnetization and (5) no suspicion of remagnetization. The quality factor does not

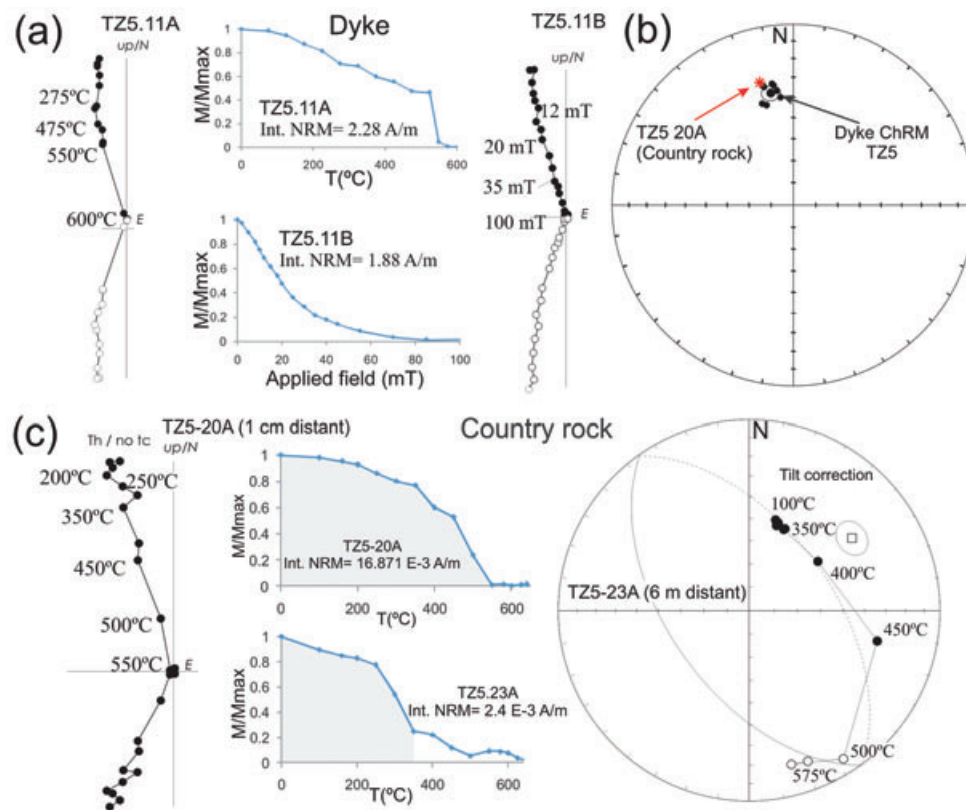


**Figure 6.** (a) Orthogonal vector diagrams and normalized magnetization decays during AF and TH demagnetization of typical IG dyke specimens (from the same sample, TZ5.11). (b) Equal area projection of specimen and site-mean directions for TZ5 IG site, including the mimic direction of the country rock sample TZ5.20 (without tilt correction). (c) Thermal demagnetization of country rock samples (TZ5.20 and TZ5.23; 1 cm and 6 m distant from the dyke margin, respectively). At increasingly distances from the IG dyke, country rocks show lower intensity NRM values and lower temperature partial thermoremanence phases (shaded area below the normalized magnetization decay); and a high unblocking temperature magnetic phase of reversed polarity, considered a pre-folding country rock ChRc, is observed.

**Table 2.** ChRc mean directions and paleomagnetic poles from Fozm Zguid (FZ), Ighrem (IG) and combined dykes (FZ+IG), and corresponding statistical parameters. *N*: number of sites; *Dec*, *Inc*: declination and inclination; *PLat*, *PLon*: pole latitude and longitude; *k*/*κ* and *α<sub>95</sub>*/*A<sub>95</sub>*: precision parameters and semi-angles of 95 per cent confidence of mean directions/paleopoles. (*Dec*, *Inc*, *α<sub>95</sub>*, *PLat*, *PLon*, *A<sub>95</sub>* in degrees).

Total	<i>N</i>	<i>Dec</i>	<i>Inc</i>	<i>k</i>	<i>α<sub>95</sub></i>	<i>PLat</i>	<i>PLon</i>	<i>κ</i>	<i>A<sub>95</sub></i>
FZ	12	336.8	39.3	127	3.9	67.9	247.9	125	3.9
IG	11	348.4	42.1	46	6.8	78.4	238.2	47	6.7
IG+FZ	23	342.2	40.8	59	4.0	73.0	244.7	55	4.1

reach the maximum value of seven due to the absence of (antipodal) reversals and (probably) to the insufficient quantity of entries and adequate statistical precision (i.e. not averaging out geomagnetic secular variation). Deenen *et al.* (2007) proposed additional statistical reliability envelope to test whether the obtained statistical parameters can be explained by paleosecular variation (PSV), defined by  $A_{95\text{min}}$  and  $A_{95\text{max}}$ . Values within this envelope can be straightforwardly explained by PSV alone, whereas values below  $A_{95\text{min}}$  likely under-represent PSV, and values above  $A_{95\text{max}}$  contain an additional source of scatter aside from PSV. The  $A_{95\text{min/max}}$  values for  $N = 11$  are  $4.6^\circ/18.1^\circ$  and for  $N = 12$   $4.4^\circ/17.1^\circ$ . The  $A_{95}$  value for IG ( $N = 11$ ,  $A_{95} = 6.7^\circ$ ) falls within this envelope, and therefore can be explained by PSV. For the FZ dyke ( $N = 12$ ,  $A_{95} = 3.9^\circ$ ), the value falls below  $A_{95\text{min}}$ , and this average therefore

does not fully represent PSV. The FZ dyke results should therefore not be treated as a separate paleopole. We will come back to this later.

Dykes emplacements were probably synchronous with the brief episode of peak volcanic activity of the CAMP (Knight *et al.* 2004; Whiteside *et al.* 2007). This is in agreement with most paleomagnetic studies carried out in the CAMP, where mostly normal polarities were found. In the neighbouring (normal polarity) Iberian Messejana-Plasencia CAMP dyke, Palencia-Ortas *et al.* (2006) found younger reversed polarities associated with minor, narrow, secondary intrusions in the main dyke, restricted to a small region of Portugal. There is no evidence, either geologically or paleomagnetically, of any subsequent intrusive event that could have influenced the magnetization of the FZ or the IG dykes.

Because of the evidence for similar ages for the IG and FZ dykes, the absence of evidence for any tectonics affecting the orientations of these dykes, and the under-representation of PSV in the FZ dyke, the *ca.* 200 Ma geomagnetic field averaged record in northwest African coordinates is better represented by combining the paleomagnetic results from both dykes. The resulting mean direction (Fig. 8a) and paleomagnetic pole which are obtained combining directions and VGPs from both dykes (IG+FZ) are:  $N = 23$ ;  $PLat = 73.0^\circ\text{N}$ ,  $PLon = 244.7^\circ\text{E}$ ,  $K = 54.9$  and  $A_{95} = 4.1^\circ$  (Table 3). The corresponding paleolatitude is  $23.7^\circ \pm 3.0^\circ$ , and the  $A_{95}$  value falls within the  $N = 23$ .  $A_{95\text{min/max}}$  envelope of  $3.4/11.4$  *sensu* Deenen *et al.* (2007), suggesting proper representation of PSV.

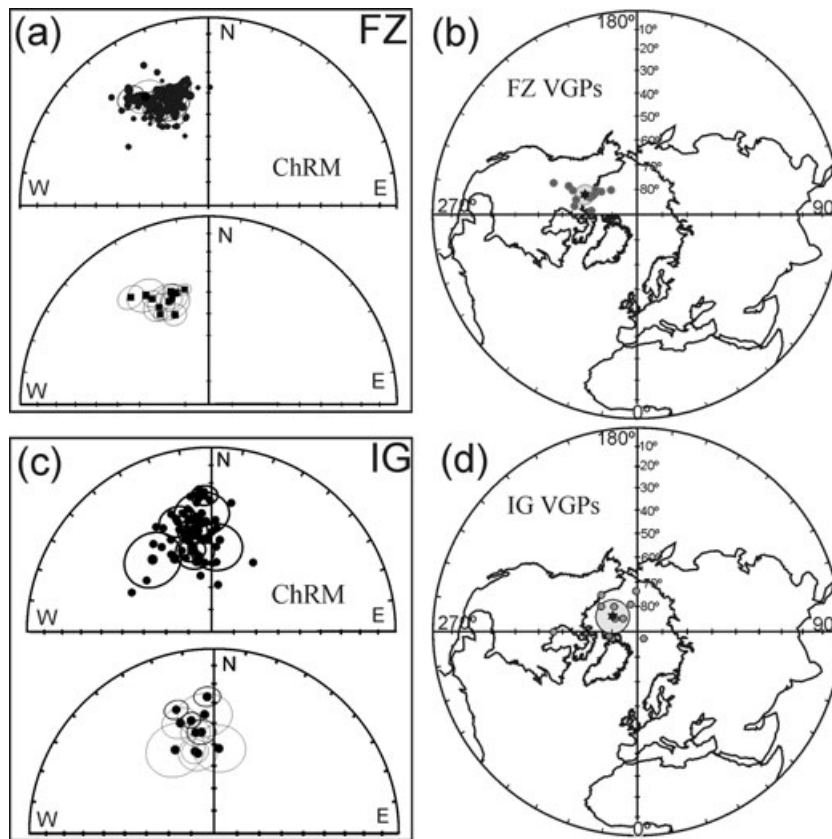


**Figure 7.** (a) Site-mean directions and (b) VGPs and paleopole of the Fom Zguid dyke on equal area projection. (c) Site-mean directions and (D) VGPs and paleopole of the Ighrem dyke on equal area projection.

**Table 3.** Paleomagnetic poles from 210 to 190 Ma igneous and sedimentary rocks of northwest Africa. *Code name:* Reference, number and name (see Fig. 9b and Table 4); *Age* (code names 8, 9, 11, 12, 13): mean age assigned in T2008; *Ref.:* Reference; *N:* number of sites; *PLat, PLon:* Pole latitude and longitude; *A<sub>95</sub>, dm, dp:* corresponding semi-angles of 95 per cent confidence. (*PLat, PLon, A<sub>95</sub>, dm, dp* in degrees).

Code name	Northwest African paleopoles (age)	<i>N</i>	<i>PLat</i>	<i>PLon</i>	<i>A<sub>95</sub></i>	Reference
1 IG	Ighrem dyke, Morocco, CAMP (200 Ma)	11	78.4	238.2	6.7	This study
2 FZ	Fom Zguid dyke, Morocco, CAMP (200 Ma)	12	67.9	247.9	3.9	This study
3 IG+FZ	Ighrem and Fom Zguid dykes, Morocco, CAMP (200 Ma)	23	73	244.7	4.1	This study
4 S2006	Fom Zguid dyke margin (200 Ma)	6	67.8	250.3	2.4	Silva <i>et al</i> (2006)
5 HM1971	Fom Zguid dyke (200 Ma)	5	58.0	259.0	4	Hailwood & Mitchell (1971)
6 T2008	T2008 running mean (200 Ma, northwest Africa)	35	69.9	236.9	3.2	Torsvik <i>et al.</i> (2008)
7 BC2002	BC2002 running mean (200 Ma, northwest Africa)	19	63.4	250.1	4.3	Besse & Courtillot (2002)
8 H1999	Freetown Complex, S. Leona, (193 Ma)	13	82.9	212.7	5.6	Hargraves <i>et al.</i> (1999)
9 B1973	Moroccan intrusives, Morocco (200 Ma)	27	71	216	7	Bardon <i>et al.</i> (1973)
10 K2004	CAMP, High Atlas, Morocco (200 Ma): ('All sites')	66	77.2	240.9	4.6	Knight <i>et al.</i> (2004)
11 M1978	Argana red beds, Morocco (200 Ma)	1(22)	50.6	251.4	12	Martin <i>et al.</i> (1978)
12 K1995	Zarzaitine Formation, Algeria (206.5 Ma)	8	70.9	235.1	2.3	Kies <i>et al.</i> (1995)
13 K2004*	CAMP, High Atlas, Morocco (200 Ma): ('Directional groups')*	5	73.0	241.3	<i>dm</i> = 18.5; <i>dp</i> = 5.0	Knight <i>et al.</i> (2004)

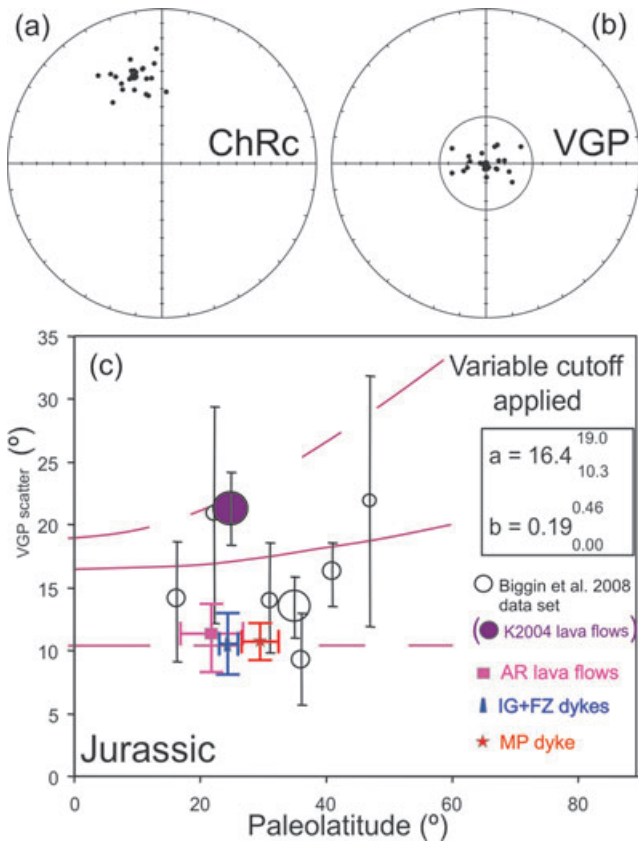


**Figure 8.** IG+FZ dyke: (a) Equal area projection of observed Characteristic Remanent components (ChRcs) directions. (b) Equal area projections of corresponding VGPs centred on their mean direction, showing that the Vandamme (1994) cut-off angle do not reject any VGP. (c) Observed IG+FZ VGP scatter, with its 95 per cent bootstrap uncertainty limits, which is integrated in the VGP dispersion curve of Biggin *et al.* (2008) for the Jurassic, where other results of variable cut-offs applied to ‘high quality’ data sets at different palaeolatitudes are shown, the shape parameters (‘a’, ‘b’) of the best-fit Model G (McFadden *et al.* 1988) with 95 per cent bootstrap uncertainty limits are given and the resulting curves plotted. VGP scatter of CAMP paleomagnetic results from the Iberian Messejana-Plasencia dyke (MP, Palencia-Ortas *et al.* 2010) and the Moroccan Argana lava flows (AR, Ruiz-Martínez *et al.* 2007) are also plotted.

## 7 DISCUSSION

### 7.1 Paleosecular variation at the T–J boundary

Although the knowledge of the angular dispersion dependence with latitude in ancient geological times is still a work in progress (e.g. Biggin *et al.* 2008), IG+FZ palaeosecular variation (PSV) has been evaluated in terms of the angular dispersion of the data set of 23 VGPs around their mean paleomagnetic pole (Fig. 8b). The total angular dispersion  $S_T$  of the IG+FZ VGPs, each being an angular distance  $\Delta$  away from the mean, was calculated (e.g. McElhinny & McFadden 1997) from  $S_T^2 = \sum \Delta_i^2 / (N - 1)$ .  $S_T$  value must be corrected (Cox 1970) by the within-site scatter  $S_W$  (a function of the mean value of  $\alpha_{95}$  for the data set  $\alpha_{95, \text{avg}}$ , the latitude  $\lambda$  and the mean value of the number of samples per site,  $n_{\text{avg}}$ ) produced by the experimental errors:  $(S_W^2 / n_{\text{avg}}) = (0.335 \alpha_{95, \text{avg}}^2) 2(1 + 3 \sin^2 \lambda) / (5 + 3 \sin^2 \lambda)$ . The geomagnetic dispersion  $S_F$  is then:  $S_F^2 = S_T^2 - (S_W^2 / n_{\text{avg}})$ .

None of the IG+FZ VGPs were rejected after applying the iterative process defined by Vandamme (1994) to obtain an optimum

cut-off angle  $\Theta = 24.7^\circ$  (which directly depend on the angular dispersion of the VGP distribution;  $\Theta = 1.8 S + 5^\circ$ ). The obtained cut-off angle is  $\Theta = 24.7^\circ$  and the maximum individual VGP distance to the mean  $20.5^\circ$ . The bootstrap method was used to evaluate upper and lower propagations of the geomagnetic dispersion uncertainty.

IG+FZ VGP dispersion ( $N = 23$ ,  $S_F = 10.5^\circ_{8.1^\circ}$ , Fig. 8) is an excellent agreement with that observed at the CAMP-related Messejana–Plasencia dyke (MP, Fig. 8) that traverses Portugal and Spain ( $N = 44$ ,  $S_F = 10.6^\circ_{9.1^\circ}$ ; Palencia-Ortas *et al.* 2010) when the 46 paleomagnetic results available for this Iberian dyke (Schott *et al.* 1981; Perrin *et al.* 1991; Palencia-Ortas *et al.* 2006) are combined after rejecting 5 sites with less than 5 samples, and their PSV analysed in the same way using the Vandamme cut-off.

IG+FZ VGP dispersion is also concordant, at its corresponding paleolatitude and considering its uncertainty, with the best-fit Model G (McFadden *et al.* 1988) fitted to the high-quality PSV results from selected Jurassic data sets of Biggin *et al.* (2008) (applying a Vandamme cut-off, in which the dependence of  $S$  with latitude differs from that observed during the last 5 Ma, Fig. 8c). This high-quality data set of Biggin *et al.* (2008) compiles results from extrusive rocks and tuffs, including Moroccan CAMP results from the High Atlas (Knight *et al.* 2004; hereafter also referred as K2004, see Fig. 8c). The K2004 data yields a much higher VGP dispersion ( $N = 40$ ,  $S_F = 21.3^\circ_{18.3^\circ}$ ) than those obtained from the rest of the Jurassic inputs (Fig. 8c), as well as from our new results obtained at similar paleolatitudes from the IG+FZ dykes ( $N = 23$ ,  $S_F = 10.5^\circ_{8.1^\circ}$ ). Biggin *et al.* (2008) noted that the K2004 data set is heavily affected by short duration bursts of volcanic activity, and Knight *et al.* (2004) hence binned their results into clustered ‘directional groups’ (numbered DG1–DG7, also based on stratigraphy and geochemistry). The K2004 input used by Biggin *et al.* (2008) is the combination of all the data from the five directional groups selected by Knight *et al.* (2004) to give a mean pole for Africa at 200 Ma (Tables 3 and 4). However, we agree that taking many data points clustered around essentially five unique, fairly separated directions will lead to an overestimation of VGP dispersion. Vandamme cut-off selection, depending on each scatter distribution, enhances these effects on the K2004 data set.

On the other hand, PSV estimates obtained from dykes may slightly underrepresent PSV, as dykes cool slower, and within each site some PSV may be averaged. We can check if the slower cooling rate of dykes than lavas may suppress the PSV scatter slightly in the dykes. Therefore, we have calculated VGP dispersion of the CAMP lava flows from the Argana basin in Morocco, preliminarily reported by Ruiz-Martínez *et al.* (2007). Resulting geomagnetic dispersion ( $N = 13$ ,  $S_F = 11.4^\circ_{8.2^\circ}$ ) is in line (AR, Fig. 8) with the results obtained from the IG+FZ and MP CAMP dykes but lower than the High Atlas K2004 input included in Biggin *et al.* (2008).

We note that the scatter values obtained from the MP Iberian dyke (Palencia-Ortas *et al.* 2010) and IG+FZ dykes and AR lava flows are within the error bars suggested by Biggin *et al.* (2008), but are consistently lower than the average graph for the Jurassic. But given the small amount of reliable data sets for PSV in the Jurassic, and because of the shape parameters and 95 per cent bootstrap uncertainty limits of the best-fit Model G (McFadden *et al.* 1988), the curve based on the Jurassic data (Biggin *et al.* 2008) is strongly influenced by the K2004 input (Fig. 8), our new data points may suggest a generally lower Jurassic PSV scatter than thus far assumed. We suggest that the MP and (IG+FZ) dykes and AR lava flows estimates (Fig. 8) yields the most reliable representation

**Table 4.** Testing indistinguishable directions (‘MM90 tests’, McFadden & McElhinny 1990) between pairs of paleopoles (see Code name) listed in Table 3. Marked column 3: IG+FZ (this study) paleopole tested against the rest (results showed in bold). Negative (–) and positive (quality A, B, C and indeterminate) results of the MM90 tests. (Ind.: indeterminate result, performed vs. *K2004\** using  $A_{95} = dm$ ).

Code name	1	2	3	4	5	6	7	8	9	10	11	12	13
1 <i>IG</i>													
2 <i>FZ</i>	–												
3 <i>IG+FZ</i>	<b>B</b>	<b>B</b>											
4 <i>S2006</i>	–	A	–										
5 <i>HM1971</i>	–	–	–	–									
6 <i>T2008</i>	–	B	<b>B</b>	–	–								
7 <i>BC2002</i>	–	B	–	B	–	–							
8 <i>H1999</i>	B	–	–	–	–	–	–						
9 <i>B1973</i>	C	–	–	–	–	B	–	–					
10 <i>K2004</i>	B	–	<b>B</b>	–	–	–	–	–	–				
11 <i>M1978</i>	–	–	–	–	C	–	C	–	–	–			
12 <i>K1995</i>	–	–	<b>B</b>	–	–	A	–	–	B	–	–		
13 <i>K2004*</i>	Ind.	Ind.	Ind.	Ind.	Ind.	Ind.	Ind.	Ind.	Ind.	Ind.	Ind.	Ind.	Ind.

of PSV for late Triassic—early Jurassic ages at the corresponding paleolatitudes.

**7.2 Comparison with the African APW 200 Ma paths and poles**

The new IG and FZ paleopoles obtained in this study have been (individually and combined) compared (Table 3, Figs 9a and b) with (i) previous preliminary studies of the FZ dyke (Hailwood & Mitchell 1971; Silva *et al.* 2006b), (ii) the 200 Ma BC2002 and T2008 ‘synthetic’ poles calculated for a 20 Ma sliding window in 10 Myr intervals, after transferring them to northwest African coordinates ( $N = 19, PLat = 63.4^\circ, PLon = 250.1^\circ, A_{95} = 4.3^\circ$  and  $N = 35, PLat = 69.9^\circ, PLon = 236.9^\circ, A_{95} = 3.2^\circ$ , respectively) and (iii) the African entries of ‘similar’ ages ( $200 \pm 10$  Ma) included in the BC2002 and T2008 compilations. The T2008 APWP contains only five paleomagnetic poles, whereas the BC2002 APWP contains no African poles of this time window. The T2008 poles were obtained from igneous (Hargraves *et al.* 1999; Bardon *et al.* 1973; Knight

*et al.* 2004) and sedimentary (Martin *et al.* 1978; Kies *et al.* 1995) rocks.

Africa has traditionally been divided into three main tectonic domains, S Africa, NE Africa and NW Africa. All individual, available analysed paleopoles of ‘similar’ ages ( $200 \pm 10$  Ma) come from the northwest Africa domain. In spite of the low value of the rotation angles involved ( $\omega < 2^\circ$ ), finite rotation poles for Gondwana used to rotate BC2002 and T2008 APWPs for South Africa onto NW Africa coordinates were respectively those used in BC2002 (Müller *et al.* 1993) and in T2008 (Nürnberg & Müller 1991).

The statistics described by McFadden & Jones (1981) and McFadden & McElhinny (1990) (hereafter denoted the ‘MM90 test’) have been used to test the hypothesis that two Fisherian distributions of individual directions share a common true mean direction at the 95 per cent confidence level (by evaluating both the angle between the two mean directions,  $\gamma_o$ , and the critical angle,  $\gamma_c$ , at which the hypothesis would be rejected), and their ‘A’, ‘B’, ‘C’ or ‘indeterminate’ quality classification (decreasing with rising values of  $\gamma_c$ :  $\gamma_c \leq 5^\circ, 5^\circ < \gamma_c \leq 10^\circ, 10^\circ \leq \gamma_c \leq 20^\circ$  and  $\gamma_c > 20^\circ$ ,

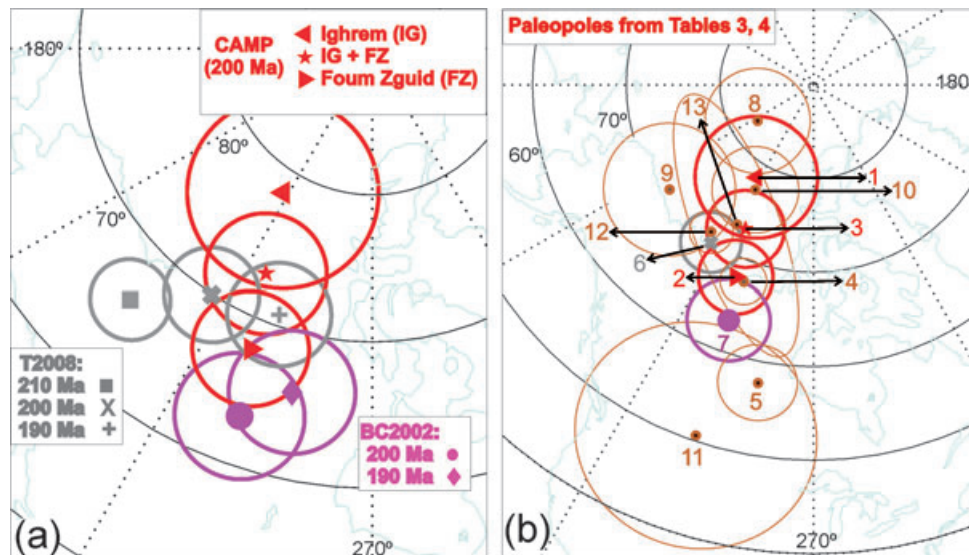


**Figure 9.** (a) Equal area projection showing IG, FZ and combined IG+FZ paleopoles comparison with similar aged trends of the BC2002 and T2008 APWPs transferred to northwest Africa. (b) Northwest African paleopoles listed in Table 3. (1) IG (this study), (2) FZ (this study), (3) IG+FZ (this study), (4) Silva *et al.* (2006b), (5) Hailwood & Mitchell (1971), (6) T2008 (Torsvik *et al.* 2008), (7) BC2002 (Besse & Courtillot 2002), (8) Hargraves *et al.* (1999), (9) Bardon *et al.* (1973), (10) ‘all sites’, Knight *et al.* (2004), (11) Martin *et al.* (1978), (12) Kies *et al.* (1995) and (13) ‘directional groups’, Knight *et al.* (2004).

respectively). MM90 tests have been performed using simulation (McFadden 1990) when the hypothesis of a common precision parameter  $k$  (Fisher 1953) failed. A summary of MM90 test results in between each pair of poles listed in Table 3 (and illustrated in Fig. 9b) is shown in Table 4.

(i) The new FZ paleopole is statistically distinct from the paleopole obtained by Hailwood & Mitchell (1971) from five FZ dyke sites. This is probably due to the incomplete demagnetization in previous study, along with the low number of sites/specimens (5/23). Conversely, the paleopole determined by Silva *et al.* (2006b) from six (fully demagnetized) FZ dyke margin sites is indistinguishable ('quality A',  $\gamma_0 = 0.9^\circ < \gamma_c = 4.9^\circ$ ) from the new paleopole—obtained from 12 sites from the central part of the dyke.

From this the following conclusions can be made: (a) despite the VRM–CRM remagnetizations affecting the dyke margin, the magnetization acquired during dyke emplacement has been partially preserved; (b) there has been no important deformation at the dyke margins and (c) there was no (paleomagnetically) significant delay in remanence acquisition between the dyke centre and its margins.

(ii) The new IG+FZ paleopole gives 'quality B' positive MM90 test results tested against the new IG and FZ individual poles ( $\gamma_0 = 5.6^\circ < \gamma_c = 8.2^\circ$  and  $\gamma_0 = 5.2^\circ < \gamma_c = 5.8^\circ$ , respectively). IG+FZ pole has been compared with other African paleopoles from those five paleomagnetic entries in the 200 ± 10 Ma age interval which have been included in BC2002 or T2008 APWPs, coming from igneous or sedimentary rocks.

One of these studies (Knight *et al.* 2004) has been duplicated in two entries accordingly with the different treatment applied by the authors to site-mean directions from 66 lavas and sediments from CAMP sections in Morocco. One pole (entry 10 in Tables 3 and 4) was calculated using all site-mean directions, which the authors considered not representative of a mean 200 Ma African pole, being distinct to the BC2002 200 Ma pole. Then, the authors identified five distinct directional groups within the lavas (associated with short periods of volcanic activity that lead to incomplete averaging of secular variation) and considered the mean of the directional groups the best way of calculating the palaeopole (entry 13 in Tables 3 and 4). Both poles are maintained here for comparisons, as the second is included in the T2008 APWP compilation although it is determined in such a subjective way and it is characterized by large 95 per cent uncertainty bounds.

MM90 tests only show indistinguishable results with the paleomagnetic data from the Late Triassic-Liasic sediments of the Zarzaitine Algerian formations (Kies *et al.* 1995) and the CAMP lavas of the Moroccan Atlas studied by Knight *et al.* (2004) when all the flows are included as individual inputs in the mean pole ('quality B',  $\gamma_0 = 3.6^\circ < \gamma_c = 5.0^\circ$  and  $\gamma_0 = 4.3^\circ < \gamma_c = 6.5^\circ$ , respectively). Comparison between the rest of individual entries (including previous FZ preliminary paleomagnetic data) and the IG+FZ pole gives negative MM90 test results. This could be attributable to a difference in age (Hargraves *et al.* 1999) or is probably due to several factors, as partial demagnetization techniques and other 'old' paleomagnetic laboratory procedures (Hailwood & Mitchell 1971; Bardon *et al.* 1973; Martin *et al.* 1978) or incomplete secular variation averaging (but not tectonic biases).

(iii) The new FZ pole lies in between BC2002 and T2008 200 Ma running means transferred to the northwest African Plate and, when it is compared with them, gives positive MM90 test results ('quality B',  $\gamma_0 = 4.6^\circ < \gamma_c = 5.9^\circ$  and  $\gamma_0 = 4.5^\circ < \gamma_c = 5.2^\circ$ , respectively). In contrast, the IG pole comparison with the BC2002 and T2008 200 Ma paleopoles gives negative MM90 test results. The T2008 200 Ma running mean is in between IG and FZ poles (Fig. 9a). So,

the combined IG+FZ pole is indistinguishable from the T2008 one ('quality B',  $\gamma_0 = 3.9^\circ < \gamma_c = 5.4^\circ$ ), but it is statistically distinct (negative MM90 test result) from the BC2002 200 Ma synthetic pole.

This discrepancy could be explained by the different kinematic models and paleomagnetic data selection criteria used in the construction of both APWPs. The T2008 200 Ma running mean is computed using 35 paleomagnetic poles mostly from North America (18) but also from Europe (6), Africa (five, all located in northwest Africa, Table 3), East Antarctica (2), Madagascar (1), South America (2) and India–Pakistan (1). The 19 paleopoles selected in BC2002 in the 20 Ma sliding window centred on 200 Ma (mean age computed from the data = 196.7 Ma) come from Antarctica (3), Australia (1), Europe (3), from BC2002 and particularly North America (12), and do not include any African paleopoles. We conclude that our new results from Morocco are in line with the APWP of T2008. Further analysis of the plate tectonic implications of our findings will be the focus of a future paper.

## 8 CONCLUSIONS

A detailed paleomagnetic study (23 sites, 188 samples included in the final analyses) of the IG and FZ dykes, which belong to the CAMP in the Anti-Atlas Ranges, Morocco, has been carried out. A stable, high unblocking temperature/coercivity, primary characteristic magnetization was recognized, supported by positive contact tests. It was readily distinguishable from low unblocking temperature/coercivity, secondary magnetizations that were principally due to a recent overprint or to lightning strikes. The magnetic mineralogy, very similar in both dykes, was dominated by single- and multidomain magnetite and low-Ti titanomagnetite, with minor contributions by oxidized magnetite and haematite.

Only normal polarities are found in IG and FZ ChRcs. IG and FZ poles are distinct one from each other in agreement with different secular variation records related with relatively short, different CAMP magmatic stages. After combining VGPs from both dykes, the geomagnetic dispersion ( $S = 10.5^{13.0^\circ}_{8.1^\circ}$ ) of the corresponding mixed distribution is in line with that observed at the Messejana-Plasencia CAMP dyke in Iberia (Palencia-Ortas *et al.* 2010) and in the Moroccan CAMP lavas of Argana basin (Ruiz-Martínez *et al.* 2007). These values for paleo-secular variation at 200 Ma are here presented as new data entries in the compilation of PSV in the Jurassic (Biggin *et al.* 2008). Our new data points significantly differ from the CAMP aged entry of this dispersion curve at the same paleolatitude and may suggest a generally lower Jurassic PSV scatter than thus far assumed. The corresponding IG+FZ paleolatitude ( $23.7^\circ \pm 3.0^\circ$ ) is concordant with North Atlantic latitudinal reconstructions of CAMP continental rift basins (Kent & Tauxe 2005). IG+FZ combined results provide a new *ca.* 200 Ma paleomagnetic pole for NW Africa ( $PLat = 73.0^\circ N$ ,  $PLon = 244.7^\circ E$ , with  $N = 23$ ,  $\kappa = 54.9$  and  $A_{95} = 4.1^\circ$ ), which has a high-quality factor following the classification scheme of Van der Voo (1990).

Statistical comparisons with the available 20 Ma running windows centred at 200 Ma of BC2002 and T2008 APWPs (in northwest Africa frame) and with poles of 'similar' ages (190–210 Ma) obtained from igneous and sedimentary rocks from the African Plate indicate dissimilar concordance results with the present IG+FZ paleopole.

The new IG+FZ pole provides an independent test of the available 200 Ma APWP running means, being in agreement with that recently proposed by T2008 and confirming the validity of the

corresponding segment obtained from paleomagnetic data of different plates (particularly influenced by North American data contribution), translated to northwest Africa through available kinematics models based on magnetic anomalies and fracture zones and realistic estimates of pre-breakup extension (T2008, and references therein).

## ACKNOWLEDGMENTS

The authors sincerely thank the helpful logistic and geological guidance of Manuel Julivert during field-trip, the help of Ricardo Palomino during field-work and also acknowledge Fort Hoofddijk Paleomagnetic Laboratory for providing the programs used in the paleomagnetic and PSV analysis. This work has been supported by the Spanish 'Dirección General de Investigación Científica y Tecnológica' DGICYT (projects BTE2002-00854, GCL2005-00211/BTE), UCM/Santander (project PR27/05-13936-BSCH) and 'Ministerio de Educación (DGES)' (project CGL2009-10840). VCRM is grateful to the MEC (Spain) 'José Castillejo Program, ref. JC2008-00356' and EEA 'Abel extraordinary chairs' for corresponding mobility grants; and to the Department of Earth Sciences of the Mohammed V-Agdal University in Rabat and the Physics of Geological Processes group of Oslo University for their hospitality during 2009 and 2010. The authors thank Bernard Henry and an anonymous reviewer for their thorough assessments, which lead to considerable improvement of the paper.

## REFERENCES

- Aarab, E.M., Rahimi, A. & Rocci, G., 1994. Un exemple de différenciation transverse: le grand dyke de Foum Zguid (Anti-Atlas, Maroc), *C. R. Acad. Sci. Paris*, **319**(II), 209–215.
- Bardon, C., Bossert, A., Hamzeh, R. & Westphal, M., 1973. Etude paléomagnétique de formations du Trias et du Jurassique du Maroc et du Sahara, *C. R. Acad. Sci. Paris*, **276**, 2357–2360.
- Bertrand, H., 1991. The Mesozoic tholeiitic province of northwest Africa: a volcano-tectonic record of the early opening of Central Atlantic, in *The Phanerozoic African Plates*, pp. 146–188, eds Kampunzu, A.B. & Lubala, R.T., Springer-Verlag, Berlin-Heidelberg.
- Bertrand, H., Dostal, J. & Dupuy, C., 1982. Geochemistry of early Mesozoic tholeiites from Morocco, *Earth planet. Sci. Lett.*, **58**, 225–239.
- Besse, J. & Courtillot, V., 2002. Apparent and true polar wander and the geometry of the magnetic field in the last 200 million years, *J. geophys. Res.*, **107**(B11), 2300, doi:10.1029/2000JB000050.
- Biggin, A.J., Van Hinsbergen, D.J.J., Langereis, C.G., Straathof, G.B. & Deenen, M.H.L., 2008. Geomagnetic secular variation in the Cretaceous Normal Superchron and in the Jurassic, *Phys. Earth planet. Inter.*, **169**, 3–19, doi:10.1016/j.pepi.2008.07.004.
- Burkhard, M., Caritg, S., Helg, U., Robert-Charrue, C. & Soulaïmani, A., 2006. Tectonics of the anti-Atlas of Morocco, *C. R. Geosci.*, **338**, 11–24.
- Cebriá, J.M., Lopez-Ruiz, J., Doblas, M., Martins, L.T. & Munhá, J., 2003. Geochemistry of the Early Jurassic Messejana-Plasencia dyke (Portugal-Spain): implications on the origin of the Central Atlantic Magmatic Province, *J. Petrol.*, **44**, 547–568.
- Cox, A., 1970. Latitude dependence of the angular dispersion of the geomagnetic field, *Geophys. J. R. astr. Soc.*, **20**, 253–269.
- Day, R., Fuller, M.D. & Schmidt, V.A., 1977. Hysteresis properties of titanomagnetites: grain size and composition dependence, *Phys. Earth planet. Inter.*, **13**, 260–266.
- Deenen, M.H.L., van Hinsbergen, D.J.J. & Langereis, C.G., 2007. The reliability of paleomagnetic directions, *EOS, Trans. Am. geophys. Un.*, **88**(52), Fall Meet. Suppl., Abstract GP33A-0919.
- Deenen, M.H.L., Ruhl, M., Bonis, N.R., Krijgsman, W., Kuerschner, W.M., Reitsma, M. & van Bergen, M.J., 2010. A new chronology for the end-Triassic mass extinction, *Earth planet. Sci. Lett.*, **291**, 113–125.
- De Min, A., Piccirillo, E.M., Marzoli, A., Bellieni, G., Renne, P.R., Ernesto, M. & Marques, L.S., 2003. The Central Atlantic Magmatic Province (CAMP) in Brazil: petrology, geochemistry,  $^{40}\text{Ar}/^{39}\text{Ar}$  ages, paleomagnetism and geodynamic implications, in *The Central Atlantic Magmatic Province: Insights from Fragments of Pangea*, pp. 91–128, doi:10.1029/136GM06, eds Hames, W.E., McHone, J.G., Renne, P.R. & Ruppel, C., Geophysical Monograph Series Volume 136, Washington, DC.
- Dunlop, D.J., 2002. Theory and application of the Day plot (Mrs/Ms versus Hcr/Hc). 1. Theoretical curves and tests using titanomagnetite data, *J. geophys. Res.*, **107**(B3), doi:10.1029/2001JB000486. EPM 4.1–4.22.
- Dunlop, D.J., Schutts, L.D., & Hale, C.J., 1984. Paleomagnetism of Archean rocks from northwestern Ontario: III. Rock magnetism of the Shelley Lake granite, Quetico Subprovince, *Can. J. Earth Sci.*, **21**, 879–886.
- Ernesto, M., Bellieni, G., Piccirillo, E.M., Marques, L.S., Pacca, I.G., Martins, G. & Macedo, J.W.P., 2003. Paleomagnetic and geochemical constraints on the timing and duration of the CAMP activity in Northeastern Brazil, in *The Central Atlantic Magmatic Province: Insights from Fragments of Pangea*, pp. 129–149, doi:10.1029/136GM06, eds Hames, W.E., McHone, J.G., Renne, P.R. & Ruppel, C., Geophysical Monograph Series Volume 136, Washington, DC.
- Fisher, R.A., 1953. Dispersion on a sphere, *Proc. Roy. Soc. Lond. Ser. A*, **217**, 295–305.
- Frizon de Lamotte, D., Leturmy, P., Missenard, Y., Khomsi, S., Ruiz, G., Saddiqi, O., Guillocheau, F. & Michard, A., 2009. Mesozoic and Cenozoic vertical movements in the Atlas system (Algeria, Morocco, Tunisia): an overview, *Tectonophysics*, **475**, 9–28, doi:10.1016/j.tecto.2008.10.024.
- Hailwood, E.A. & Mitchell, J.G., 1971. Paleomagnetic and radiometric dating results from the Jurassic intrusions in South Morocco, *Geophys. J. R. astr. Soc.*, **24**, 351–364.
- Hargraves, R.B., Briden, J.C. & Daniels, B.A., 1999. Palaeomagnetism and magnetic fabric in the Freetown Complex, Sierra Leone, *Geophys. J. Int.*, **136**, 705–713.
- Henry, B., Merabet, N.E., Derder, M.E.M. & Bayou, B., 2004. Chemical remagnetizations in the Illizi basin (Algeria), *Geophys. J. Int.*, **156**, 200–212.
- Jasonov, P.G., Nourgaliev, D.K., Burov, B.V. & Heller, F., 1998. A modernized coercivity spectrometer, *Geol. Carpathica*, **49**, 224–226.
- Kent, D.V. & Tauxe, L., 2005. Corrected Late Triassic latitudes for continents adjacent to the North Atlantic, *Science*, **307**(5707), 240–244.
- Kies, B., Henry, B., Merabet, N., Derder, M.M. & Daly, L., 1995. A new Late Triassic-Liasic palaeomagnetic pole from superimposed and juxtaposed magnetizations in the Saharan craton, *Geophys. J. Int.*, **120**, 433–444.
- Kirschvink, J.J., 1980. The least-squares line and plane and the analysis of paleomagnetic data, *Geophys. J. R. astr. Soc.*, **62**, 699–718.
- Knight, K.B., Nomade, S., Renne, P.R., Marzoli, A., Bertrand, H. & Youbie, N., 2004. The Central Atlantic Magmatic Province at the Triassic–Jurassic boundary: paleomagnetic and  $^{40}\text{Ar}/^{39}\text{Ar}$  evidence from Morocco for brief, episodic volcanism, *Earth planet. Sci. Lett.*, **228**, 143–160.
- Labails, C., Olivet, J.L., Aslanian, D. & Roest, W.R., 2010. An alternative early opening scenario for the Central Atlantic Ocean, *Earth planet. Sci. Lett.*, **297**(3–4), 355–368.
- Leblanc, M., 1973. Le grand dyke de dolérite de l'Anti-Atlas et le magmatisme jurassique du Sud Marocain, *C. R. Acad. Sci. Paris*, **t.276**, série D, 2943–2946.
- Lowrie, W., 1990. Identification of ferromagnetic minerals in a rock by coercivity and unblocking temperature properties, *Geophys. Res. Lett.*, **17**, 159–162.
- Marcais, J. & Choubert, G., 1956. *Les grands traits de la géologie du Maroc. Lexique stratigraphique du Maroc, introduction géologique*, Direction des Mines et de la Géologie, Rabat.
- Martin, D.L., Nairn, A.E.M., Noltimier, H.C., Petty, M.H. & Schmidt, T.J., 1978. Paleozoic and Mesozoic paleomagnetic results from Morocco, *Tectonophysics*, **44**, 91–114.
- Marzoli, A., Renne, P.R., Piccirillo, E.M., Ernesto, M., Bellieni, G., & De Min, A., 1999. Extensive 200-million-year-old continental flood basalts of the Central Atlantic magmatic province, *Science*, **284**, 616–618.

- Marzoli, A. *et al.*, 2004. Synchrony of the Central Atlantic magmatic province and the Triassic-Jurassic boundary climatic and biotic crisis, *Geology*, **32**, 973–976.
- May, R.P., 1971. Pattern of Jurassic-Triassic diabase dikes around the North Atlantic in the context of predrift position of the continents, *Geol. Soc. Am. Bull.*, **82**, 1285–1292.
- McElhinny, M.W. & McFadden, P.L., 1997. Palaeosecular variation over the past 5 Myr based on a new generalized database, *Geophys. J. Int.*, **131**, 240–252.
- McFadden, P.L., 1990. A new fold test for palaeomagnetic studies, *Geophys. J. Int.*, **103**, 163–169.
- McFadden, P.L. & Jones, F.J., 1981. The discrimination of mean directions drawn from Fisher distributions, *Geophys. J. R. astr. Soc.*, **67**, 19–33.
- McFadden, P.L. & McElhinny, M.W., 1988. The combined analysis of remagnetization circles and direct observations in paleomagnetism, *Earth planet. Sci. Lett.*, **87**, 161–172.
- McFadden, P.L. & McElhinny, M.W., 1990. Classification of the reversal test in paleomagnetism, *Geophys. J. Int.*, **103**, 725–729.
- McFadden, P.L., Merrill, R.T. & McElhinny, M.W., 1988. Dipole/quadrupole family modeling of paleosecular variation, *J. geophys. Res.*, **93**, 11 583–11 588.
- Michard, A., 1976. Eléments de Géologie Marocaine, *Notes Mem. Serv. Géol. Maroc*, **252**, 7–408.
- Müller, D.M., Royer, J.Y. & Lawver, L.A., 1993. Revised plate motions relative to the hotspots from combined Atlantic and Indian Ocean hotspot tracks, *Geology*, **21**, 275–278.
- Nomade, S., Knight, K.B., Renne, P.R., Verati, C., Féraud, G., Marzoli, A., Youbi, N. & Bertrand, H., 2007. The chronology of CAMP: relevance for the central Atlantic rifting processes and the Triassic–Jurassic biotic crisis, *Palaeogeogr. Palaeoclimatol. Palaeoecol.*, **244**, 326–344.
- Nürnberg, D. & Müller, R.D., 1991. The tectonic evolution of the South Atlantic from Late Jurassic to present, *Tectonophysics*, **191**, 27–53, doi:10.1016/0040-1951(91)90231-G.
- Olsen, P.E., Kent, D.V., Et-Touhami, M. & Puffer, J.H., 2003. Cyclo-, magneto-, and bio-stratigraphic constraints on the duration of the CAMP event and its relationship to the Triassic-Jurassic boundary, in *The Central Atlantic Magmatic Province: Insights from Fragments of Pangea*, pp. 7–32, doi:10.1029/136GM02, eds Hames, W.E., McHone, J.G., Renne, P.R. & Ruppel, C., Geophysical Monograph Series Volume 136, Washington, DC.
- Palencia-Ortas, A., 2004. *Estudio Paleomagnético de rocas de edad Jurásica de La Península Ibérica y Sur de Marruecos*, ISBN: 84-669-2865-0, Ph.D. thesis, Universidad Complutense de Madrid, Madrid.
- Palencia-Ortas, A., Osete, M.L., Vegas, R. & Silva, P., 2006. Paleomagnetic study of the Messejana Plasencia dyke (Portugal and Spain): a lower Jurassic paleopole for the Iberian plate, *Tectonophysics*, **420**, 455–472.
- Palencia-Ortas, A., Ruiz Martínez, V.C. & Osete, M.L., 2010. Analysis of the Jurassic geomagnetic dispersion recorded by the Iberian magmatism and preliminary palaeomagnetic data of Jurassic volcanic rocks from the southeast Iberian Ranges, *Fis. Tierra*, **22**, 35–58.
- Perrin, M., Prevot, M. & Mankinen, E.A., 1991. Low intensity of the geomagnetic field in early Jurassic time, *J. geophys. Res.*, **96**(9), 14 197–14 210.
- Ruiz-Martínez, V.C., Villalain, J.J. & Palencia-Ortas, A., (2007). Paleomagnetic and AMS results of Late Triassic red beds, CAMP-related lava flows and Lower Jurassic limestones from Argana Basin, Morocco: Geodynamic implications, in *Earth: Our Changing Planet. Proceedings of IUGG XXIV General Assembly Perugia, Italy 2007 (LAGA ASI002 Symposium 'Paleomagnetism and geodynamics neotectonics, continental reconstruction, reference frames')*, 3047, (p. 68), compiled by L. Ubertini, P. Manciola, S. Casadei, S. Grimaldi, www.iugg2007perugia.it.
- Sebai, A., Feraud, G., Bertrand, H. & Hanes, J., 1991.  $^{40}\text{Ar}/^{39}\text{Ar}$  dating and geochemistry of tholeiitic magmatism related to the early opening of the central Atlantic rift, *Earth planet. Sci. Lett.*, **104**, 455–472.
- Schermerhorn, L.J.G., Priem, H.N.A., Boelrijk, N.A.I.M., Hebeda, E.H., Verdurmen, E.A.T. & Verschure, R.H., 1978. Age and origin of the Messejana dolerite fault-dyke system (Portugal and Spain) in light of opening of North Atlantic Ocean, *J. Geol.*, **86**, 299–309.
- Schoene, B., Bartolini, A., Schaltegger, U. & Blackburn, T.J., 2010. Correlating the end-Triassic mass extinction and flood basalt volcanism at the 100 ka level, *Geology*, 38–5, 387–390, doi:10.1130/G30683.1.
- Schott, J.J., Montigny, R. & Thuizat, R., 1981. Paleomagnetism and potassium-argon age of the Messejana dyke (Portugal and Spain): angular limitation to the rotation of the Iberian Peninsula since the middle Jurassic, *Earth planet. Sci. Lett.*, **53**, 457–470.
- Silva, P.F., Marques, F.O., Henry, B., Mateus, A., Lourenco, N. & Miranda, J.M., 2004. Preliminary results of a study of magnetic properties in the Foun-Zguid dyke (Morocco), *Phys. Chem. Earth*, **29**, 909–920.
- Silva, P.F., Henry, B., Marques, F.O., Mateus, A., Madureira, P., Lourenco, N. & Miranda, J.M., 2006a. Variation of magnetic properties in sedimentary rocks hosting the Foun Zguid dyke (southern Morocco): Combined effects of re-crystallization and Fe-metasomatism, *Earth planet. Sci. Lett.*, **241**, 978–992.
- Silva, P.F., Henry, B., Marques, F.O., Madureira, P. & Miranda, J.M., 2006b. Paleomagnetic study of the great Foun Zguid Dyke (southern Morocco); a positive contact test related to metasomatic processes, *Geophys. Res. Lett.*, **33**(21), L21301, doi:10.1029/2006GL027498.
- Stacey, F.D., 1967. The Koenigsberger ratio and the nature of thermoremanence in igneous rocks, *Earth planet. Sci. Lett.*, **2**, 67–68.
- Thomas, R.J., Fekkak, A., Ennih, N., Errami, E., Loughlin, S.C., Gresse, P.G., Chevallier, L.P. & Liégeois, J.-P., 2004. A new lithostratigraphic framework for the Anti-Atlas Orogen, Morocco, *J. Afr. Earth Sci.*, **39**, 217–226.
- Torsvik, T.H., Müller, R.D., Van Der Voo, R., Steinberger, B. & Gaina C., 2008. Global plate motion frames: toward a unified model, *Rev. Geophys.*, **46**, RG3004, doi:10.1029/2007RG000227.
- Touil, A., Vegas, R., Hafid, A., Palomino, R., Rizki, A., Palencia-Ortas, A. & Ruiz-Martínez, V.C., 2008. Petrography, mineralogy and geochemistry of the Ighrem diabase dyke (Anti-Atlas, Southern Morocco), *Rev. Soc. geol. España*, **21**(1–2), 25–33.
- Vandamme, D.A., 1994. A new method to determine paleosecular variation, *Phys. Earth planet. Inter.*, **85**, 131–142.
- Van Der Voo, R., 1990. The reliability of paleomagnetic data, *Tectonophysics*, **184**, 1–9.
- Verati, C., Rapaille, C., Féraud, G., Marzoli, A., Bertrand, H. & Youbi, N., 2007.  $^{40}\text{Ar}/^{39}\text{Ar}$  ages and duration of the Central Atlantic Magmatic Province volcanism in Morocco and Portugal and its relation to the Triassic–Jurassic boundary, *Palaeogeogr. Palaeoclimatol. Palaeoecol.*, **244**, 308–325.
- Whiteside, J.H., Olsen, P.E., Kent, D.V., Fowell, S.J. & Et-Touhami, M., 2007. Synchrony between the Central Atlantic magmatic province and the Triassic–Jurassic mass-extinction event?, *Palaeogeogr. Palaeoclimatol. Palaeoecol.*, **244**, 345–367.
- Youbi, N., Tavares Martins, L., Munhá, J.M., Ibouh, H., Madeira, J., Ait Chayeb, E.H. & El Boukhari, A., 2003. The Late Triassic–Early Jurassic Volcanism of Morocco and Portugal in the framework of the Central Atlantic Magmatic Province: an overview, in *The Central Atlantic Magmatic Province: Insights from Fragments of Pangea*, pp. 179–207, doi:10.1029/136GM06, eds Hames, W.E., McHone, J.G., Renne, P.R. & Ruppel, C., Geophysical Monograph Series Volume 136, Washington, DC.